Electrochemistry

The Electrochemical Society of Japan

Received: August 29, 2018
Accepted: September 27, 2018
Published online: November 23, 2018

https://doi.org/10.5796/electrochemistry.18-00068

Article

*Electrochemistry*, **87(1)**, 47–51 (2019)

# Protein-Engineering Improvement of Direct Electron Transfer-Type Bioelectrocatalytic Properties of D-Fructose Dehydrogenase

**Yuya HIBINO, Shota KAWAI, Yuki KITAZUMI, Osamu SHIRAI, and Kenji KANO***

*Division of Applied Life Sciences, Graduate School of Agriculture, Kyoto University, Sakyo, Kyoto 606-8502, Japan*

* *Corresponding author: kano.kenji.5z@kyoto-u.ac.jp*

## ABSTRACT

D-Fructose dehydrogenase (FDH) contains a flavin adenine dinucleotide (FAD) in subunit I and three heme *c* moieties (1*c*, 2*c*, and 3*c* from the N-terminus) as the electron transfer relaying sites. The electron transfer in direct electron transfer-type bioelectrocatalysis of FDH is proposed to proceed in sequence from FAD, through heme 3*c*, to heme 2*c* without going through heme 1*c*. In order to improve the performance of the bioelectrocatalysis, we constructed a variant (M450QΔ1*c*FDH) in which 143 amino acid residues involving heme 1*c* were removed and M450 as the sixth axial ligand of heme 2*c* was replaced with glutamine to negatively shift the formal potential of heme 2*c*. The M450QΔ1*c*FDH variant was adsorbed on a planar gold electrode. The variant-adsorbed electrode produced a clear sigmoidal steady-state catalytic wave of fructose oxidation in cyclic voltammetry. The limiting current density was 1.4 times larger than that of the recombinant (native) FDH. The half-wave potential of the wave shifted by 0.2 V to the negative direction. M450QΔ1*c*FDH adsorbed rather homogeneously in orientations suitable for DET-type bioelectrocatalysis.



Keywords : Fructose Dehydrogenase, Direct Electron Transfer, Downsizing, Redox Potential Shift

## 1. Introduction

Direct electron transfer- (DET-) type bioelectrocatalysis is a coupled reaction of a redox enzymatic reaction and an electrode reaction without mediators.[1–11] DET-type bioelectrocatalysis is attracting significant attention for construction of mediatorless biosensors and biofuel cells and for fundamental analysis of redox properties of enzymes.[12,13] In DET-type bioelectrocatalysis, the redox active site in the adsorbed enzyme directly communicates with electrodes. However, there is a limit to the number of enzymes that show clear DET-type catalytic activity, since the redox active sites are in many cases embedded in the insulating peptide of the enzyme.[14]

Our group has been focusing on D-fructose dehydrogenase (FDH) from *Gluconobacter japonicus* NBRC 3260 as a model enzyme of DET-type bioelectrocatalysis.[15,16] FDH is a membrane-bound enzyme that produces DET-type catalytic wave of fructose oxidation in large current densities.[17–19] A biofuel cell with DET-type bioelectrocatalysis using FDH on the anode exhibited a high power density (2.6 mW cm$^{-2}$ under quiescent conditions).[20] FDH is a heterotrimeric enzyme complex that consists of subunits I (67 kDa), II (51 kDa), and III (20 kDa).[21] Subunit I has one covalently bound flavin adenine dinucleotide (FAD) at which D-fructose is oxidized. Subunit II has three heme *c* moieties as the electron transfer relaying sites: heme 1*c* with M301 as the sixth axial ligand, heme 2*c* with M450, and heme 3*c* with M578 from the N-terminus. The electron transfer in the DET reaction of FDH is proposed to proceed in sequence from the FAD, through heme 3*c*, to heme 2*c* (as the electron-donating site to electrodes) without going through heme 1*c*[23,24] (Fig. 1(A)). Subunit III plays a key role in the expression of FDH.[22–25]

For improvement of the DET-type bioelectrocatalysis, several enzyme modification approaches were attempted:[26] (i) trimming of the N- or C-terminals and deglycosylation to reduce the size of enzymes and to open up the redox active site,[27–30] (ii) site-directed mutagenesis at the redox active site to change its redox and catalytic characteristics,[31,32] and (iii) addition of the tag sequences to control the orientation of enzymes.[28,33]

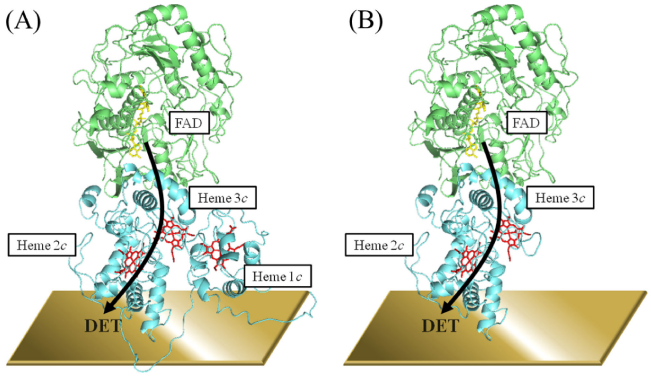


**Figure 1.** Schematic of orientations suitable for DET-reaction of FDH and M450QΔ1*c*FDH-variant based on homology modeling. Structural data of FAD-glucose dehydrogenase from *Aspergillus flavus* (PDB 4YNT) and thiosulfate dehydrogenase from *Marichromatium purpuratum* "isolated" (PDB 5LO9) were used as templates of subunits I (green) and II (blue), respectively, in the homology modeling. The small subunit III was not considered in the modeling for lack of structural information of similar enzymes.

In this study, we attempted to take two strategies in order to improve the performance of the DET-type bioelectrocatalysis of FDH: (a) trimming of the N-terminal to reduce the enzyme size and (b) site-directed mutation to decrease the overpotential. For this purpose, we designed a variant M450QΔ1*c*FDH in which 143 amino acid residues involving heme 1*c* were removed, and M450 as the sixth axial ligand of heme 2*c* was replaced with glutamine to shift the formal potential of heme 2*c* to the negative potential side. As a result, M450QΔ1*c*FDH-adsorbed electrode exhibited high current density and small overpotential compared to the recombinant (native) FDH-adsorbed electrode in DET-type bioelectrocatalysis. We also discuss conceivable electrostatic interaction between M450QΔ1*c*FDH and charged electrode surface.

## 2. Experimental

### 2.1 Materials

Herculase II fusion DNA polymerase and restriction endonucleases were purchased from Agilent Technologies (Santa Clara, CA) and Takara Shuzo (Japan), respectively. DNA ligase was obtained from Toyobo (Japan). Potassium ferricyanide was obtained from Nakalai Tesque (Japan). Other chemicals were obtained from Wako Pure Chemical Industries (Japan).

### 2.2 Preparation of the mutants and FDH

To prepare the M450QΔ1*c*FDH variant, two mutations were introduced to the *fdh* gene of the plasmid pSHO13 that was used for expressing the recombinant (native) FDH.[22] pSHO13 is a broad-host-range vector pBBR1-MCS4[34] inserted with a fragment of a putative promoter region of the *adhAB* gene of *G. oxydans* 621H and a fragment of the complete $fdh_{ATG}$ gene. The site-directed mutation M450Q was introduced to the *fdh* gene by inverse polymerase chain reaction (PCR) using primers fdhC_heme2*c*Gln(+) (5′-ACAGGCAGAAGCAATCGAGCATAGCC-3′) and fdhC_heme2*c*(−) (5′-GGTCCTGCTGCACGAGCATGTG-3′). An in-frame deletion of the region containing the heme 1*c* moiety was introduced by PCR using primers fdhC_AARIEGK(+) (5′-GCGGCAAGAATCGAAGGCAAACCC-3′) and fdhC_SignalTerminal(−) (5′-TTGCGCCCGTACGTTCGTCCCTGC-GAG-3′). All nucleotide sequences of the $fdh_{ATG}$ gene of the PCR products were confirmed by Fasmac Sequencing Service (Japan).

*G. oxydans* NBRC 12528 Δ*adhA*::Km$^r$ was transformed with the mutation-introduced pSHO13, as described in a previous paper.[35] *Gluconobacter* cells were cultivated, and then the recombinant (native) FDH and M450QΔ1*c*FDH as well as M450QFDH (a variant with glutamine in place of methionine of the sixth axial ligand of heme 2*c*) and Δ1*c*FDH (a variant lacking 143 amino acid residues from the N-terminus) were purified as described in previous papers[22,25] with some little modifications as described below. All enzymes were solubilized only for 1 h at 4°C. The elution of Δ1*c*FDH and M450QΔ1*c*FDH from a DEAE-sepharose column was carried out using a concentration gradient of McIlvain buffers (McB) at pH 6.0 from 20-fold-diluted McB to 5-fold-diluted McB containing 1 mM 2-mercaptoethanol and 0.1% (w/v) TritonX-100 (M = mol dm$^{-3}$).

Since the crystal structure of FDH remains unknown, homology modeling was done using the crystal structural data of already characterized FAD-glucose dehydrogenase from *Aspergillus flavus* (PDB 4YNT) for subunit I and thiosulfate dehydrogenase from *Marichromatium purpuratum* "isolated" (PDB 5LO9) for subunit II were used as templates, as described in a previous paper.[19]

### 2.3 Electrochemical measurements

Cyclic voltammetry and linear sweep voltammetry were performed on an ALS 611s voltammetric analyzer under anaerobic conditions. Polycrystalline Au electrodes were used as the working electrodes. The Au electrode was polished to a mirror-like finish with $Al_2O_3$ powder (0.02 µm particle size), rinsed with distilled water, and sonicated in distilled water. The reference and counter electrodes were a handmade Ag|AgCl|sat.KCl electrode and Pt wire, respectively. All potentials are referred to the reference electrode in this paper. Cyclic voltammograms (CVs) were recorded at 25°C at a scan rate ($v$) of 10 mV s$^{-1}$ in 1.0 mL of McB (pH 4.5) that contained 0.2 M D-fructose (L = dm$^3$). For measurements of DET-type catalytic waves, a 3 µL aliquot of the enzyme solution was added to the buffer solution. As a result, the electrolysis solution contained 6 µM 2-mercaptoethanol and 3 ppm (w/v) TritonX-100.

### 2.4 Other analytical methods

The FDH activity was spectrophotometrically measured with potassium ferricyanide (as an electron acceptor) and the ferric dupanol regent, as described in the literature.[21]

## 3. Results and Discussion

The M450QΔ1*c*FDH variant was successfully constructed. The concentrations of the recombinant (native) FDH and M450QFDH were spectrophotometrically determined using the absorption coefficient of the reduced heme *c* at 550 nm ($\varepsilon_{550nm}$ = 23,000 M$^{-1}$ cm$^{-1}$).[36] The concentration of Δ1*c*FDH and M450QΔ1*c*FDH were evaluated by assuming that the absorption coefficient of the variants is two-thirds of that of the recombinant (native) FDH, since Δ1*c*FDH and M450QΔ1*c*FDH have two heme *c* moieties, while FDH has three hemes *c*. Before the electrochemical measurements, all enzyme solutions were diluted with a 50 mM phosphate buffer containing 1 mM 2-mercaptoethanol and 0.1% (w/v) TritonX-100, and the concentrations of the enzymes were adjusted to that of M450QΔ1*c*FDH (7.7 µM). The enzyme activity was evaluated as follows: $2.0 \times 10^{10}$ U mol$^{-1}$ for the recombinant (native) FDH, $1.8 \times 10^{10}$ U mol$^{-1}$ for M450QFDH, $1.2 \times 10^{10}$ U mol$^{-1}$ for Δ1*c*FDH, and $1.3 \times 10^{10}$ U mol$^{-1}$ for M450QΔ1*c*FDH.

Characterizations of the recombinant (native) FDH- and variant-adsorbed electrodes were performed by linear sweep voltammetry in the presence of D-fructose. Each of the enzymes was physically adsorbed on a bare Au electrode. Clear DET-type catalytic waves corresponding to D-fructose oxidation were observed at all of the enzymes-adsorbed electrodes. The current-potential curves were not affected by stirring (Fig. S1). Therefore, the catalytic currents are controlled by the enzyme kinetics and the interfacial electron transfer.[37–41]

In order to characterize the variants, it is important to compare the limiting catalytic current density ($j_{lim}$) independent of the electrode potential at sufficiently positive potentials. However, measurements at positive potentials more than 0.5 V cause a decrease in the catalytic currents due to a formation of Au oxide layer.[24,39] Therefore we measured the steady-state catalytic current density at 0.5 V and used it as $j_{lim}$ in this study. Additionally, we defined the apparent half-wave potential ($E_{1/2}$) of the catalytic wave as the potential to satisfy $j = j_{lim}/2$.

Figure 2 shows the linear sweep voltammograms of the recombinant (native) FDH- and variant-adsorbed electrodes in the presence of D-fructose. $E_{1/2}$ in the M450QFDH-adsorbed electrode was shifted by approximately 0.18 V in the negative direction from that in the FDH-adsorbed electrode. The $j_{lim}$ value at the Δ1*c*FDH-adsorbed electrode was about 1.6 times higher than that at the FDH-adsorbed electrode; $j_{lim}$ values were 0.31 ± 0.01 mA cm$^{-2}$ and 0.20 ± 0.01 mA cm$^{-2}$ for Δ1*c*FDH and the recombinant (native)

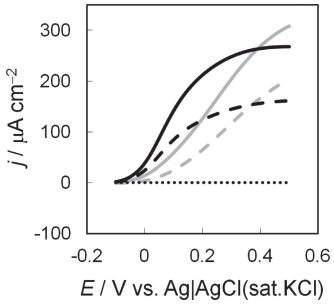


**Figure 2.** Linear sweep voltammogram of D-fructose oxidation at the recombinant (native) FDH- (dashed gray line), M450QFDH- (dashed black line), Δ1*c*FDH- (gray line), and M450QΔ1*c*FDH- (black line) adsorbed electrodes in McB (pH 4.5) in the presence of 0.2 M D-fructose under anaerobic conditions at $v$ = 10 mV s$^{-1}$. The dotted line indicates the background at the bare Au electrode.

FDH, respectively, in three repeated experiments. It is considered that the negative direction shift of $E_{1/2}$ is attributed to a negative direction shift of the redox potential of the electron-donating site, and that the increased current density is attributed to an increase in the surface concentration of the enzymes on the electrodes.[24,25]

The M450Q$\Delta$1*c*FDH-adsorbed electrode exhibited both of the effects of the mutations. $E_{1/2}$ in the M450Q$\Delta$1*c*FDH-adsorbed electrode was shifted by approximately 0.20 V in the negative direction from that in the FDH-adsorbed electrode. Moreover, $j_{lim}$ in the M450Q$\Delta$1*c*FDH-adsorbed electrode ($0.27 \pm 0.01$ mA cm$^{-2}$) was about 1.4 times higher than that in the FDH-adsorbed electrode. In contrast, the solution activity of M450Q$\Delta$1*c*FDH ($1.3 \times 10^{10}$ U mol$^{-1}$) measured with $[Fe(CN)_6]^{3-}$ as an electron acceptor was smaller than that of the recombinant (native) FDH ($2.0 \times 10^{10}$ U mol$^{-1}$).

Originally, electrode potential- and scan rate (or convection)-independent $j_{lim}$ should be completely controlled by the enzyme kinetics and is given by:[37–42]

$$j_{lim} = n_s F k_{cat} \Gamma \quad (1)$$

where $n_s$ is the number of electrons of the substrate, $F$ is the Faraday constant, $k_{cat}$ is the catalytic constant, and $\Gamma$ is the surface concentration of "electrochemically efficient" enzymes. $k_{cat}$ in Eq. (1) is different from the solution activity that depends on electron acceptors. However, we may assume that $k_{cat}$ is proportional to the solution activity of a given electron acceptor. On the assumption, it is expected that the increase in $j_{lim}$ of M450Q$\Delta$1*c*FDH is attributed to an increase of $\Gamma$ corresponding due to the downsizing protein engineering of the enzyme:

$$\frac{\Gamma_{M450Q\Delta1cFDH}}{\Gamma_{FDH}} = \frac{j_{lim,M450Q\Delta1cFDH}}{j_{lim,FDH}} \Big/ \frac{k_{cat,M450Q\Delta1cFDH}}{k_{cat,FDH}} \approx 1.4/0.65 \cong 2.2 \quad (2)$$

The M450QFDH- and M450Q$\Delta$1*c*FDH-adsorbed electrodes exhibited clear sigmoidal shape in the steady-state catalytic waves; the catalytic currents of the M450QFDH- and M450Q$\Delta$1*c*FDH-adsorbed electrodes reached the limiting value at potentials as negative as 0.4 V. The characteristics are in strong contrast with the catalytic waves of the FDH- and $\Delta$1*c*FDH-electrodes; the catalytic waves increased almost linearly with the electrode potential. The increase is called "residual slope" and is caused by the random orientation of the enzymes adsorbed on an electrode surface.[2,37,38] Therefore, it is concluded that M450QFDH and M450Q$\Delta$1*c*FDH rather homogeneously adsorbed on the Au electrode in orientations convenient for the DET-type bioelectrocatalysis.

We assumed orientations most suitable for DET-reaction of FDH and M450Q$\Delta$1*c*FDH, respectively, as shown in Fig. 1. In our proposed orientations, we considered facing subunit II to the electrode surface and locating heme 2*c* in a vertical angle to the electrode, by considering that FDH is a membrane-bound enzyme. As judged from the proposed orientations and structures of FDH and M450Q$\Delta$1*c*FDH, it can be expected that the downsizing protein engineering of the enzyme leads to a decrease in the occupied area of the adsorbed enzyme and an increase in the compactness in the (homogeneous) orientation. In addition, the random orientation of FDH leads to a decrease in $\Gamma$ of the effective enzyme on the electrode, and to an underestimation of $j_{lim}$, because clear limiting current was not recorded for the recombinant (native) FDH in the potential range investigated. All these factors seem to be able to explain the factor of 2.2 in Eq. (2).

Here we may point out some singular behaviors of the M450Q$\Delta$1*c*FDH variant in DET-type bioelectrocatalytic reaction. When the variant was adsorbed at open circuit potential and the electrode potential was scanned from −0.3 V to 0.5 V, the catalytic wave in the forward positive-going scan was smaller than that in the backward negative-going scan in the first cycle (Fig. 3(A)): during the potential scan, the orientation of the variant seems to be improved at positive potential region. Such hysteresis characteristics were weakened in the second cycle. When the electrode potential was scanned from −0.1 V to 0.5 V, only weak hysteresis characteristics were observed in the first cycle, but not in the second cycle (Fig. 3(B)). Similar characteristics were also observed for the M450Q variant, but not for the recombinant (native) FDH and $\Delta$1*c*FDH. Therefore, we considered that such hysteresis characteristics were due to some electrostatic interaction between the electrode and the variants with M450Q (variants of which M450 as the sixth axial ligand of heme 2*c* was replaced with glutamine): the variants with M450Q stably and homogeneously adsorb at positively charged electrode surface, but some electrostatic repulsion may occur at negative potentials.

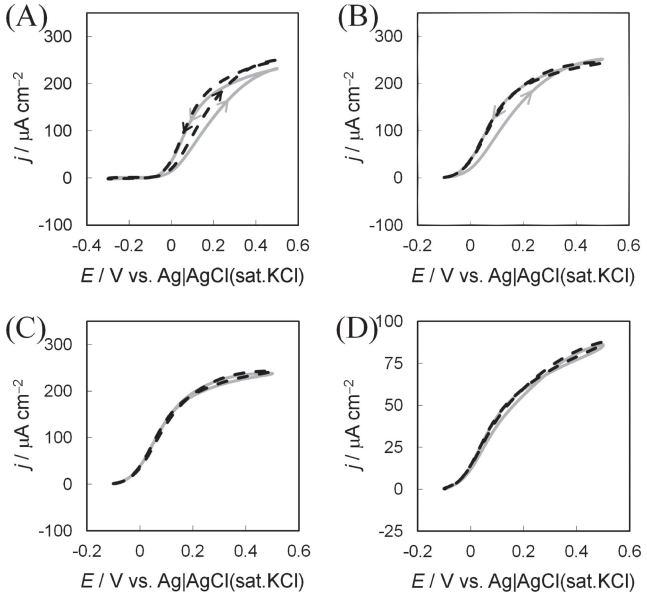


**Figure 3.** CVs of D-fructose oxidation at M450Q$\Delta$1*c*FDH-adsorbed Au electrodes in McB (pH 4.5) in the presence of 0.2 M D-fructose under anaerobic conditions at $v = 10$ mV s$^{-1}$. (A) CV in scanning from −0.3 V after adsorption of the variant at the open circuit potential. The gray line is the first scan, and the dashed black line is the second scan. (B) CV in scanning from −0.1 V. The other conditions are identical with those of (A). (C) CV after adsorption of the variant at 0.5 V. The other conditions are identical with those of (B). (D) CV after the following treatments: the variant was adsorbed at the open circuit potential, and the potential was scanned 2 cycles from −0.1 V to 0.5 V. Thereafter, the electrode was held at −0.3 V for 5 min, and then transferred to a fresh electrochemical solution (McB, pH 4.5) containing 0.2 M D-fructose.

In order to verify our hypothesis, additional experiments were done. When M450Q$\Delta$1*c*FDH was adsorbed at 0.5 V, clear steady-state sigmoidal waves were observed without any hysteresis in the scan from −0.1 V (Fig. 3C). In contrast, when the M450Q$\Delta$1*c*FDH-adsorbed electrode was hold at −0.3 V for 3 min and transferred to a fresh electrolysis solution containing D-fructose, the catalytic wave decreased drastically (Fig. 3D), most probably due to the desorption of the variant from the negatively charged electrode surface. Such change in the catalytic wave was observed at M450QFDH-adsorbed electrode, but not at the FDH- and $\Delta$1*c*FDH-adsorbed electrode: the catalytic wave of the FDH- and $\Delta$1*c*FDH-adsorbed electrode remained almost unchanged after holding at −0.3 V and transferring to a fresh electrolysis solution.

The positively and negatively charged amino acid residues almost homogeneously distribute on the surface of FDH (Fig. S2). In addition, hydrophobic and hydrophilic residues also distribute

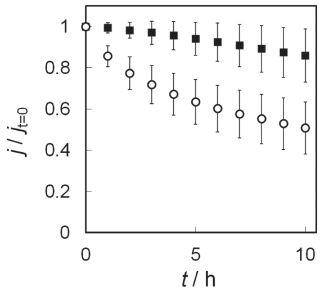


**Figure 4.** Stability of the recombinant (native) FDH (closed squares) and M450QΔ1*c*FDH (open circles) adsorbed on bare Au electrodes at 25°C in McB (pH 4.5) in the presence of 0.2 M D-fructose. The normalized values of $j_{lim}$ obtained from the second cycle CVs taken every one hour were plotted. The error bar was evaluated using Student's *t*-distribution at a 90% confidence level in three repeated experiments.

homogeneously (Fig. S3). These properties seem to lead to random orientation of FDH on Au electrodes, although we have to also consider some other contributions from 2-mercaptoethanol[43] and TritonX-100[44] on the orientation for further discussion.

On the other hand, the M450Q mutation (for M450QΔ1*c*FDH and M450Q) was introduced near heme 2*c*. Several negatively charged amino acid residues such as Glu and Asp exist around heme 2*c* (Fig. S4). Therefore, it may be considered that the M450Q mutation induces the electrostatic repulsion between Glu at 450 and the other negatively charged amino acid residues around heme 2*c*, which causes slight change in the conformation to increase the negative potential charge on the surface near heme 2*c*. Since the heme 2*c* moiety in M450QΔ1*c*FDH and M450Q is considered to face to the electrode surface rather homogeneously (Fig. 1(B), some electrostatic repulsion may cause partial desorption from the electrode at negative potentials. However, the adsorbed M450QΔ1*c*FDH and M450Q are stabilized at positive potentials.

Finally, effects of the protein engineering on the enzyme stability were investigated by recording $j_{lim}$ every one hour at 0.5 V as a measure of the stability. Figure 4 shows the normalized values of $j_{lim}$ observed at the FDH- and M450QΔ1*c*FDH-adsorbed electrode in the presence of D-fructose. The $j_{lim}$ of the FDH- and M450QΔ1*c*FDH-adsorbed electrode decreased with time approximately 1% and 8% per hour, respectively. The two mutations resulted in a slight decrease in the stability of the enzyme, although they improved the bioelectrocatalytic property of the enzyme. The M450QΔ1*c*FDH mutation would disturb the balance between hydrophobic and hydrophilic properties on the enzyme surface, which may causes some structural change in the variant.

## 4. Conclusions

We have successfully constructed and purified a variant of M450QΔ1*c*FDH that lacks 143 amino acid residues involving the heme 1*c* moiety and has glutamine in place of methionine as the sixth axial ligand of heme 2*c*. The linear sweep voltammogram of D-fructose oxidation at M450QΔ1*c*FDH-adsorbed electrode exhibited a large limited current density and a negative direction shift of $E_{1/2}$ compared to that at the FDH-adsorbed electrode. Moreover, it is suggested that the M450QΔ1*c*FDH is rather homogeneously adsorbed in orientations suitable for DET-type bioelectrocatalysis. It is considered that the negative direction shift of $E_{1/2}$ is attributed to a negative direction shift of the redox potential of heme 2*c* as the electron-donating site in the DET reactions and to the improved interfacial electron transfer kinetics due to homogeneous orientation suitable for DET reactions. The large current is attributed to an increase in the surface concentration of the enzyme on an electrode due to downsizing. This is the first report to support the idea that the effects of the two types of the mutations are rather simply additive even under drastic mutation. Unexpected but effective effects of the mutation is that the variants with M450Q stably and homogeneously adsorb at positively charged electrode surface compared with the recombinant (native) FDH and Δ1*c*FDH. Therefore, the strategy of mixed type mutations is useful for improving the properties of the DET-type bioelectrocatalysis of other redox enzymes, and the variant may be applicable to constructing high power biofuel cells and sensitive biosensors under suitable conditions. Further strategy of the mutation required in future will be to improve the stabilization.

## Supporting Information

The Supporting Information is available on the website at DOI: https://doi.org/10.5796/electrochemistry.18-00068.

## Acknowledgments

This work was supported by Research Fellowships of Japan Society for the Promotion of Science for Young Scientists (to Y. H., #201708760).

## References

1. S. V. Hexter, T. F. Esterle, and F. A. Armstrong, *Phys. Chem. Chem. Phys.*, **16**, 11822 (2014).
2. C. Léger and P. Bertrand, *Chem. Rev.*, **108**, 2379 (2008).
3. R. D. Milton and S. D. Minteer, *J. R. Soc. Interface*, **14**, 20170253 (2017).
4. N. Mano and A. de Poulpiqet, *Chem. Rev.*, **118**, 2392 (2018).
5. D. Leech, P. Kavanagh, and W. Schuhmann, *Electrochim. Acta*, **84**, 223 (2012).
6. S. Calabrese Barton, J. Gallaway, and P. Atanassov, *Chem. Rev.*, **104**, 4867 (2004).
7. R. Ludwig, R. Ortiz, C. Schulz, W. Harreither, C. Sygmund, and L. Gorton, *Anal. Bioanal. Chem.*, **405**, 3637 (2013).
8. N. Mano and L. Edembe, *Biosens. Bioelectron.*, **50**, 478 (2013).
9. M. Sensi, M. del Barrio, C. Baffert, V. Fourmond, and C. Léger, *Curr. Opin. Electrochem.*, **5**, 135 (2017).
10. I. Mazurenko, X. Wang, A. de Poulpiquet, and E. Lojou, *Sustainable Energy Fuels*, **1**, 1475 (2017).
11. K. Sakai, H. Xia, Y. Kitazumi, O. Shirai, and K. Kano, *Electrochim. Acta*, **271**, 305 (2018).
12. W. Zhang and G. Li, *Anal. Aci.*, **20**, 603 (2004).
13. T. Ikeda, *Electrochim. Acta*, **82**, 158 (2012).
14. A. A. Karyakin, *Bioelectrochemistry*, **88**, 70 (2012).
15. T. Ikeda, F. Matsushita, and M. Senda, *Biosens. Bioelectron.*, **6**, 299 (1991).
16. Y. Kamitaka, S. Tsujimura, N. Setoyama, T. Kajino, and K. Kano, *Phys. Chem. Chem. Phys.*, **9**, 1793 (2007).
17. Y. Kamitaka, S. Tsujimura, and K. Kano, *Chem. Lett.*, **36**, 218 (2007).
18. H. Xia, Y. Hibino, Y. Kitazumi, O. Shirai, and K. Kano, *Electrochim. Acta*, **218**, 41 (2016).
19. P. Bollella, Y. Hibino, K. Kano, L. Gorton, and R. Antiochia, *Anal. Bioanal. Chem.*, **410**, 3253 (2018).
20. K. So, S. Kawai, Y. Hamano, Y. Kitazumi, O. Shirai, M. Hibi, J. Ogawa, and K. Kano, *Phys. Chem. Chem. Phys.*, **16**, 4823 (2014).
21. M. Ameyama, E. Shinagawa, K. Matsushita, and O. Adachi, *J. Bacteriol.*, **145**, 814 (1981).
22. S. Kawai, M. Tsutsumi, T. Yakushi, K. Kano, and K. Matsushita, *Appl. Environ. Microbiol.*, **79**, 1654 (2013).
23. S. Kawai, T. Yakushi, K. Matsushita, Y. Kitazumi, O. Shirai, and K. Kano, *Electrochem. Commun.*, **38**, 28 (2014).
24. Y. Hibino, S. Kawai, Y. Kitazumi, O. Shirai, and K. Kano, *Electrochem. Commun.*, **67**, 43 (2016).
25. Y. Hibino, S. Kawai, Y. Kitazumi, O. Shirai, and K. Kano, *Electrochem. Commun.*, **77**, 112 (2017).
26. G. Güven, R. Prodanovic, and U. Schwaneberg, *Electroanalysis*, **22**, 765 (2010).
27. K. Kataoka, H. Komori, Y. Ueki, Y. Konno, Y. Kamitaka, S. Kurose, S. Tsujimura, Y. Higuchi, K. Kano, D. Seo, and T. Sakurai, *J. Mol. Biol.*, **373**, 141 (2007).
28. G. Presnova, V. Grigorenko, A. Egorov, T. Ruzgas, A. Lindgren, L. Gorton, and T. Börchers, *Faraday Discuss.*, **116**, 281 (2000).
29. O. Courjean, F. Gao, and N. Mano, *Angew. Chem., Int. Ed.*, **48**, 5897 (2009).
30. R. Ortiz, H. Matsumura, F. Tasca, K. Zahma, M. Samejima, K. Igarashi, R. Ludwig, and L. Gorton, *Anal. Chem.*, **84**, 10315 (2012).

31. G. Battistuzzi, M. Borsari, J. A. Cowan, A. Ranieri, and M. Sola, *J. Am. Chem. Soc.*, **124**, 5315 (2002).
32. Y. Kamitaka, S. Tsujimura, K. Kataoka, T. Sakurai, T. Ikeda, and K. Kano, *J. Electroanal. Chem.*, **601**, 119 (2007).
33. V. Balland, C. Hureau, A. M. Cusano, Y. Liu, T. Tron, and B. Limoges, *Chem. Eur. J.*, **14**, 7186 (2008).
34. M. E. Kovach, P. H. Elzer, D. S. Hill, G. T. Robertson, M. A. Farris, R. M. Roop, and K. M. Peterson, *Gene*, **166**, 175 (1995).
35. D. H. Figurski and D. R. Helinski, *Proc. Natl. Acad. Sci. U.S.A.*, **76**, 1648 (1979).
36. J. Marcinkeviciene and G. Johansson, *FEBS Lett.*, **318**, 23 (1993).
37. C. Léger, A. K. Jones, S. P. J. Albracht, and F. A. Armstrong, *J. Phys. Chem. B*, **106**, 13058 (2002).
38. C. Léger, A. K. Jones, W. Roseboom, S. P. J. Albracht, and F. A. Armstrong, *Biochemistry*, **41**, 15736 (2002).
39. Y. Sugimoto, Y. Kitazumi, O. Shirai, and K. Kano, *Electrochim. Acta*, **170**, 242 (2015).
40. H. Xia, Y. Kitazumi, O. Shirai, and K. Kano, *J. Electroanal. Chem.*, **763**, 104 (2016).
41. K. So, Y. Kitazumi, O. Shirai, and K. Kano, *J. Electroanal. Chem.*, **783**, 316 (2016).
42. Y. Sugimoto, Y. Kitazumi, O. Shirai, and K. Kano, *Electrochemistry*, **85**, 82 (2017).
43. Y. Sugimoto, Y. Kitazumi, O. Shirai, M. Yamamoto, and K. Kano, *Electrochim. Acta*, **170**, 242 (2015).
44. S. Kawai, T. Yakushi, K. Matsushita, Y. Kitazumi, O. Shirai, and K. Kano, *Electrochim. Acta*, **152**, 19 (2015).